CAMBRIDGE
UNIVERSITY PRESS

**RESEARCH ARTICLE**

# Dating the beginning of urbanization in Central Mexico: a high-resolution chronology of the Middle Formative Period at Tlalancaleca

Tatsuya Murakami[1] [iD], Alexander Jurado[1] and Shigeru Kabata[2]

[1]Department of Anthropology, Tulane University, 6823 St Charles Ave, Dinwiddie Hall 101, New Orleans, LA 70118 USA and [2]International Research Institute for Studies in Language and Peace, Kyoto University of Foreign Studies, Kyoto, Japan
**Corresponding author:** Tatsuya Murakami; Email: tmurakam@tulane.edu

**Abstract**
Research by the Tlalancaleca Archaeological Project (PATP) has corroborated modifications to the Middle Formative chronology in Puebla-Tlaxcala (Lesure et al. 2006, 2014) using Bayesian modeling on 26 radiocarbon dates from Tlalancaleca. The present study is the first to evaluate the region's Middle Formative chronology with radiocarbon dates from superposed stratigraphy. Nine Bayesian models were constructed with different combinations of radiocarbon dates and OxCal's phase and sequence functions to determine the beginning and end of the Texoloc phase. Results place the Tlatempa-Texoloc transition at around 650 cal BC and the Texoloc-Tezoquipan transition at around 500 cal BC. The OxCal Interval function supports a timespan of approximately 150 years for the duration of the Texoloc phase. These results suggest the process of initial urbanization in Central Mexico was a rapid one.

## Introduction

The Middle Formative period (ca. 1000–500 BC) featured major social transformations in Central Mexico. Agriculture and sedentary lifeways spread from its southern to northern regions (Grove 2000; Lesure et al. 2006) and large settlements emerged in the Basin of Mexico and Puebla-Tlaxcala Valley that would later develop into urban centers (Carballo 2016; García Cook 1981; Plunket and Uruñuela 2012; Sanders et al. 1979). Understanding these important transformations requires pinpointing accurately and precisely the timing of changes in settlement and material culture. An impediment to this end has been the Hallstatt Plateau (e.g., Jacobsson et al. 2018), a plateau on the radiocarbon calibration curve spanning the Middle Formative. As a result, all true dates between 800 and 400 BC yield radiocarbon year ages around 2450 BP. Reducing the range of any single date is difficult, especially if comparing radiocarbon dates with no direct stratigraphic superposition. Through our research at Tlalancaleca, Central Mexico (Figure 1), we have investigated Middle Formative occupations and acquired a series of radiocarbon samples and dates from superposed occupation levels that span this period (Murakami et al. 2017a). These data are the basis of a high-resolution chronology for the Middle Formative. In this article, we present detailed descriptions of the stratigraphy, sample provenience, and radiocarbon dates underlying this chronology. Second, we present the Bayesian models (e.g., Bayliss et al. 2007; Beramendi-Orosco et al. 2009; Manning et al. 2006) used to narrow samples' calibrated calendar year ranges and pinpoint transition dates between phases. We consider the implications of this chronology for the timing of initial settlement at Tlalancaleca and the first pulses of population nucleation and urbanization.
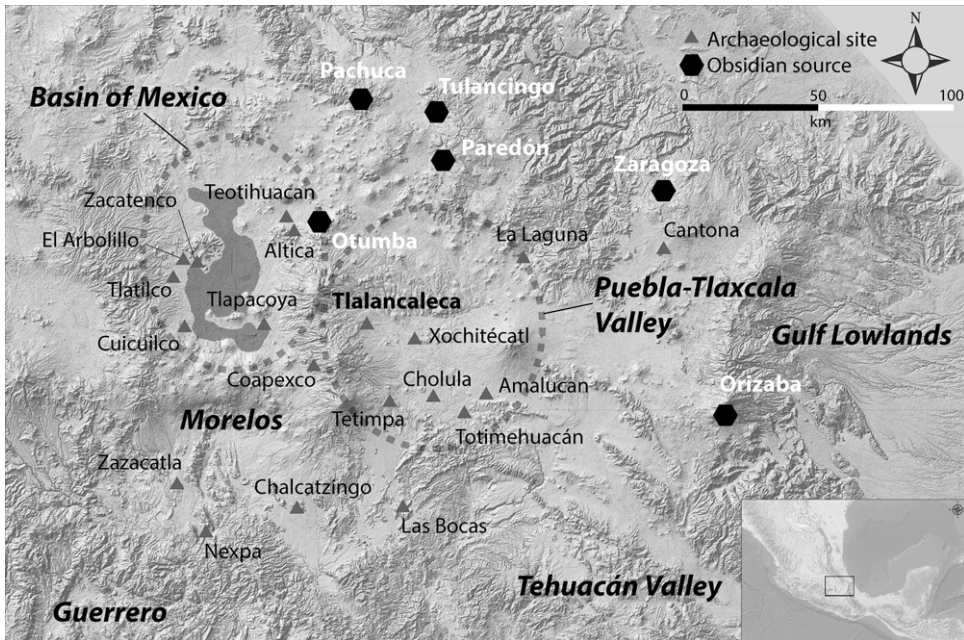
**Figure 1.** *Map of Central Mexico showing important Formative-period sites and obsidian sources.*

## Background

### Ceramic chronology in the Puebla-Tlaxcala Valley

The Puebla-Tlaxcala Valley is located in Central Mexico and adjoins the Basin of Mexico on the eastern side of its prominent volcanoes, the Popocatepetl and Iztaccihuatl (Figure 1). Pioneering work by Ángel García Cook (1972, 1974, 1976, 1981; García Cook and Merino Carrión 1997; García Cook and Merino Carrión 2005; see also Snow 1969) established the first comprehensive chronology for the region. García Cook defined four major ceramic complexes and cultural phases for the Formative period: Tzompantepec (1700/1600–1200 BC), Tlatempa (1200–800 BC), Texoloc (800–350 BC), and Tezoquipan (350 BC–AD 100) (dates are uncalibrated calendar years). The Tzompantepec phase marked the appearance of sedentary, agricultural villages in the region. These villages increased in size and number during the subsequent Tlatempa phase (García Cook 1981, 245–248). The Texoloc phase marked the onset of urbanization as García Cook (1981, 257) identified the development of five "great towns" or "cities", one of which was Tlalancaleca. Intensification of urban processes continued through the Tezoquipan phase as the number of great towns increased to 20 and they individually increased in size. This cultural sequence and ceramic chronology were based on seriated surface collections and test excavations at a select number of sites (García Cook 1972, 1974, 1976).

Richard Lesure and colleagues (2006, 2014) corroborated García Cook's ceramic complexes and phase sequence through excavations and analysis of pit features at village sites in central Tlaxcala. However, they made substantial modifications to the absolute dates of the phases, resulting in: Tzompantepec (900–800 cal BC); Tlatempa (800–650 cal BC); and Texoloc (650–500 cal BC). The basis of these changes was radiocarbon dated samples from pit features (none of which were stratigraphically superposed) and concordant changes in ceramic and figurine types between the Puebla-Tlaxcala Valley and Basin of Mexico. They supported their modifications with calibrated dates from earlier work in the Basin of Mexico (Tolstoy 1978), yet these early samples and dates are still undergoing reevaluations (Murakami 2022). Our research at Tlalancaleca (Murakami et al. 2017a) has recently corroborated the absolute dates proposed by Lesure and colleagues for the Middle Formative phases and firmly placed the onset of urbanization in the Puebla-Tlaxcala Valley in the Texoloc phase (650–500 cal BC).
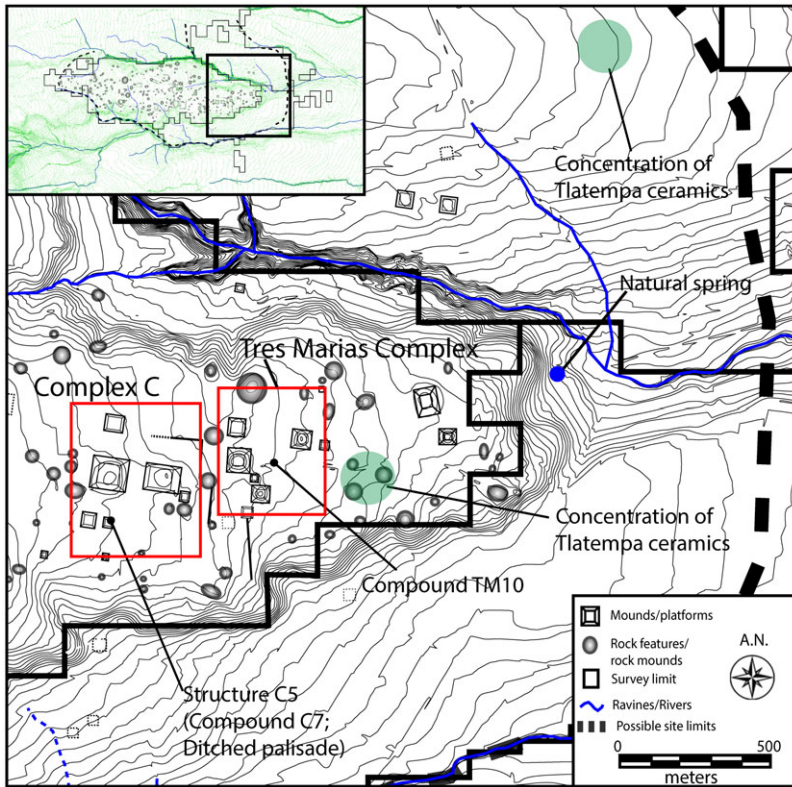
**Figure 2.** *Site map of Tlalancaleca showing the location of Complex C and Tres Marias Complex.*

### Tlalancaleca

Tlalancaleca is located on a low-lying plateau in the northeastern foothills of the Iztaccihuatl volcano (Figure 1). Results from our survey, surface collections, and excavations (Murakami et al. 2017a) indicate that the first sedentary inhabitants of Tlalancaleca formed dispersed residential groups during the Tlatempa phase (800–650 cal BC), which amounted to no more than 5 hectares in occupied area. During the Texoloc phase (650–500 cal BC), population nucleation increased the size of Tlalancaleca to at least 80 hectares (Murakami et al. 2017a). This settlement was concentrated in the eastern limits and surrounding area of the plateau (Figure 2). We have not identified monumental structures pertaining to this phase, yet we suspect they exist, concealed within the fill of posterior structures as is the case at Xochitécatl (Serra Puche et al. 2004). The urbanization process accelerated during the Tezoquipan and early Tenanyecac phases (500 cal BC–250 cal AD; Late and Terminal Formative periods) as Tlalancaleca reached its maximum area (ca. 500 hectares) and nine monumental architectural complexes were constructed across the plateau. Processes of decline and depopulation at the site began around 250 cal AD, leading to a complete hiatus in occupation during the Classic period.

## Materials and methods

Fieldwork at Tlalancaleca has yielded radiocarbon samples (all wood charcoals) from primary contexts that include burials, bell-shaped pits, other pit features, and clay amalgam (coating of buildings). In this section, we describe the architectural complexes that have yielded occupation levels from the Middle Formative period (i.e., the Tlatempa and Texoloc phases). Phase assignation of each feature (and consequently, sample) is based on preliminary ceramic analysis. Ceramic phases are discrete spatio-temporal entities built through the classification of ceramic sherds and so we recognize that they are our

analytical constructs, which might have corresponded to changes in other aspects of material culture and society or not. Our observations during excavations lead us to believe that ceramic changes broadly corresponded to changes in the use of space at the architectural complexes at Tlalancaleca described below. All samples were dated at the University of Arizona Accelerator Mass Spectrometry (AMS) Laboratory following their established methods and protocols (see Burr et al. 2007; Donahue et al. 1990).

### Excavations and samples at Complex C

Complex C is located 700 m west of the plateau's eastern edge (Figure 2). Its most prominent structures are two monumental platforms from the Terminal Formative period. Smaller, less conspicuous platforms from the Late and Terminal Formative periods are also located around them. We conducted trench and horizontal excavations to investigate one of these platforms, Structure C5. Preserved within and below this platform were occupation levels from the Tlatempa and Texoloc phases (Murakami et al. 2018, 2019). When these levels and building phases are considered together, Structure C5 presented a continuous occupation sequence from the Tlatempa through Tenanyecac phase.

The Tlatempa phase (Level 1) occupation level featured a ditched palisade or wooden enclosure. The ditch measured 0.8 m in width and 1.5 m in depth and contained post holes spaced at ca. 20 cm intervals along its interior (Figure 3). The exposed portion suggested this feature was circular and had a diameter of 10–15 m. Its function is not entirely clear but given its unique form, we think use in suprahousehold, community-level activities was more likely than use in individual household-level activities. Its construction on relatively higher terrain, removed from and overlooking the dispersed residential groups to the east, seems to support this interpretation.

The second occupation level featured Compound C7, a multi-room compound built over the ditched palisade during the Texoloc phase. We use the designations C7a-d to distinguish the structures that composed it as its rooms and spatial layout were modified repeatedly throughout the phase (Figure 3). Compound C7's earliest structures were of masonry construction and evidenced by one alignment roughly 1.5 m in length (Structure C7d) and a rectilinear and curved wall (Structure C7c-Sub1) (Levels 2a–c) (Figure 3). The latter was subsequently used as fill for a low masonry platform, Structure C7c (Level 2d), built on top. Structure C7c had a small, central staircase leading to a patio (approximately 6 x 6 m) on its southern edge. The patio was bordered by several rooms constructed of stone, adobe, and wattle and daub (Structure C7a). Structure C7c was demolished and covered by an earthen floor to support an ancillary room (Structure C7b; Level 2e) added to the north side of Structure C7a. This dynamic construction sequence produced a series of superposed floors and hemispherical pits associated with Structures C7a-d. Compound C7's functions might have been equally dynamic and until the material analysis is advanced, we refrain from designating it a residential, public, or ritual space. Compound C7 was eventually cleaned of its contents and razed in a large conflagration, possibly a termination ritual. The third occupation level featured Structure C5-Sub2, a Tezoquipan-phase masonry platform, which utilized the remnants of Compound C7 as fill. This platform was enlarged and modified several times throughout the Tezoquipan and Tenanyecac phases.

We collected 13 radiocarbon samples (all wood charcoal) from the Middle Formative contexts (one of these samples was excluded from the analysis; see below). Four samples came from fill within the ditch of the wooden enclosure (Table 1; Figure 3). The fill consisted of five natural strata, perhaps corresponding to different depositional processes. While the fill did not constitute a primary context, it was sealed by a series of Texoloc-phase floors, which allowed us to temporally assign the samples to the Tlatempa phase. We collected: one sample (AA-110686) from the bottom-most layer of fill (IIId), two samples (AA-110687 and AA-110688) from the middle layers (IIIa, b), and one sample (AA-110689) from a post hole (IV) (see Supplementary Materials for stratigraphic profiles). The post hole did not reach the bottom of the ditch but was instead superposed over an older one. This means it likely replaced an earlier post from the series lining the ditch interior and represents the most recent deposit.
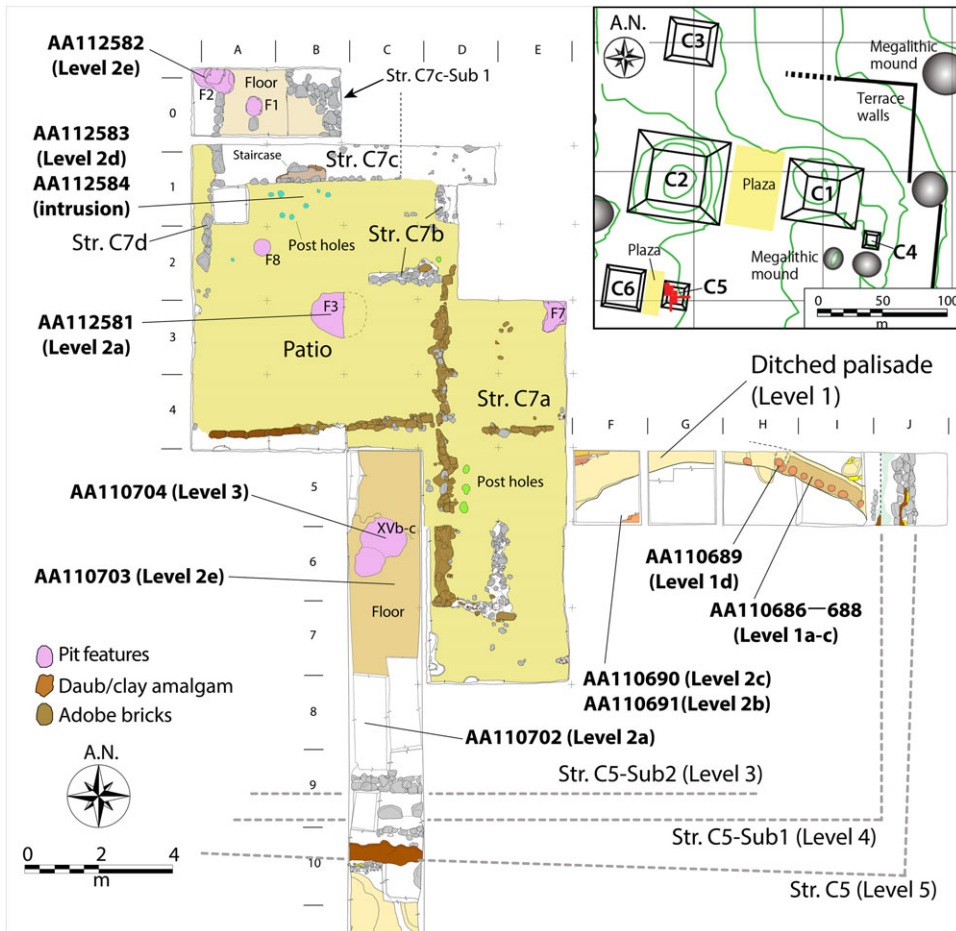
**Figure 3.** *Map of Complex C showing the spatial organization of Compound C7, the location of the ditched palisade, and the provenience of radiocarbon samples.*

Nine samples came from the five superposed levels (Levels 2a–e; Table 1; see Supplementary Materials for stratigraphic profiles) associated with Compound C7: two samples (AA-110702 and AA-112581) from pit features dug into the earliest floor (Level 2a); one sample (AA-110691) from the second floor (Level 2b); one sample (AA-110690) from near a hearth on the third floor (Level 2c); one sample (AA-112583) from the fill (sealed by a floor) covering Structure C7c (Level 2d); one sample (AA-110703) from the upper-most floor and one sample (AA-112582) from a pit feature dug from this level (Level 2e). We collected Sample AA-110704 from a pit feature dug into a Texoloc floor, but it turned out to be an outlier among our samples yielding a calibrated date range in the Late Formative (see below). We concluded this feature was dug or disturbed from a "younger" occupational level and therefore omitted Sample AA-110704 from the Texoloc samples (instead, we grouped it with the Tezoquipan phase; see below). We collected and excluded Sample AA-112584 from subsequent analysis because of its low carbon yields (~20%) that might have resulted in a non-reliable radiocarbon age.

We acquired three Tezoquipan phase samples. We collected two of these samples from Tezoquipan contexts at Complex C: Sample AA-110693 came from a floor associated with an early construction phase (Structure C5-Sub1) of the civic-ceremonial platform, Structure C5; and Sample AA-110704

**Table 1.** *Results of $^{14}C$ measurement for samples used in this study (more likely 1σ and 2σ date ranges are in bold)*

| Lab# | Sample ID | Provenience | Context | %C | δ$^{13}$C (‰) | $^{14}$C age BP | Calibrated calendar yrs (1 sigma) | P | Calibrated calendar yrs (2 sigma) | P |
|---|---|---|---|---|---|---|---|---|---|---|
| *Tlatempa Phase* | | | | | | | | | | |
| AA110686 | FB-C2E-507 | Complex C (Cala 2E[I5], Layer IIIa) | Ditched palisade, upper fill (**Level 1c**) | 56 | −25.6 | 2495 ± 20 | 758-745 BC | 7.1% | 771-721 BC | 18.6% |
| | | | | | | | 690-679 BC | 6.6% | 707-662 BC | 19.1% |
| | | | | | | | 672-665 BC | 3.9% | **652-543 BC** | 57.7% |
| | | | | | | | **645-551 BC** | 50.7% | | |
| AA110687 | FB-C2E-510 | Complex C (Cala 2E[I5], Layer IIIb) | Ditched palisade, lower fill (**Level 1b**) | 62 | −23.2 | 2453 ± 20 | **746-690 BC** | 29.6% | 751-684 BC | 31.8% |
| | | | | | | | 665-644 BC | 10.5% | 669-634 BC | 13.2% |
| | | | | | | | 551-481 BC | 28.2% | 622-613 BC | 1.3% |
| | | | | | | | | | **591-453 BC** | 43.0% |
| | | | | | | | | | 447-416 BC | 6.2% |
| AA110688 | FB-C2E-521 | Complex C (Cala 2E[I5], Layer IIId) | Ditched palisade, bottom-most layer (**Level 1a**) | 62 | −22.5 | 2437 ± 22 | 724-707 BC | 8.1% | 748-688 BC | 19.9% |
| | | | | | | | 663-652 BC | 5.4% | 666-642 BC | 8.2% |
| | | | | | | | **544-458 BC** | 44.6% | **567-409 BC** | 67.4% |
| | | | | | | | 441-419 BC | 10.2% | | |
| AA110689 | FB-C2F-463 | Complex C (Cala 2F[H5], Layer IV) | Ditched palisade, upper post hole (**Level 1d**) | 58 | −23.1 | 2456 ± 20 | **747-689 BC** | 31.3% | 753-682 BC | 33.7% |
| | | | | | | | 665-643 BC | 11.1% | 669-631 BC | 14.1% |
| | | | | | | | 565-513 BC | 21.0% | 625-610 BC | 2.2% |
| | | | | | | | 501-486 BC | 4.9% | **593-456 BC** | 40.8% |
| | | | | | | | | | 444-417 BC | 4.7% |
| *Texoloc Phase (Complex C)* | | | | | | | | | | |
| AA110690 | FB-C2H-479 | Complex C (Cala 2H[F5], Layer V) | Compound C7, Floor 3 near hearth (**Level 2c**) | 68 | −22.4 | 2511 ± 19 | 770-749 BC | 14.7% | 776-737 BC | 20.4% |
| | | | | | | | 686-667 BC | 13.6% | 695-662 BC | 18.4% |
| | | | | | | | **639-587 BC** | 34.0% | **649-546 BC** | 56.6% |
| | | | | | | | 581-570 BC | 6.0% | | |
| AA110691 | FB-C2H-501 | Complex C (Cala 2H[F5], Layer VII) | Compound C7, beneath the penultimate floor (**Level 2b**) | 62 | −24.0 | 2492 ± 19 | 756-743 BC | 7.5% | 769-720 BC | 18.4% |
| | | | | | | | 692-680 BC | 7.0% | 708-662 BC | 19.3% |
| | | | | | | | 670-665 BC | 3.1% | **653-543 BC** | 57.8% |
| | | | | | | | 646-607 BC | 23.6% | | |

| | | | | | | | | | | |
|---|---|---|---|---|---|---|---|---|---|---|
| AA110702 | FB-C3H-585 | Complex C (Cala 3H[C8], Layer VIIId) | Compound C7, pit feature (**Level 2a**) | 64 | −22.0 | 2443 ± 19 | 596-550 BC 27.1% | | | |
| | | | | | | | 733-696 BC 18.5% | 749-687 BC 24.5% | | |
| | | | | | | | 663-650 BC 7.5% | 666-641 BC 10.0% | | |
| | | | | | | | **546-472 BC** 38.2% | **569-412 BC** 61.0% | | |
| | | | | | | | 434-424 BC 4.1% | | | |
| AA110703 | FB-C3J-257 | Complex C (Cala 3J[C6], Layer Ib) | Compound C7, Floor (**Level 2e**) | 60 | −23.4 | 2515 ± 20 | 772-750 BC 17.2% | 777-740 BC 21.8% | | |
| | | | | | | | 685-667 BC 14.1% | 694-663 BC 18.4% | | |
| | | | | | | | **636-588 BC** 33.4% | **648-547 BC** 55.2% | | |
| | | | | | | | 579-572 BC 3.6% | | | |
| AA110704[*1] | FB-C3J-518 | Complex C (Cala 3J[C6], Layer XVb) | Compound C7, pit feature | 56 | −25.3 | 2267 ± 19 | **390-359 BC** 44.8% | **395-352 BC** 51.4% | | |
| | | | | | | | 276-261 BC 13.8% | 288-227 BC 42.3% | | |
| | | | | | | | 244-234 BC 9.7% | 219-210 BC 1.7% | | |
| AA112581 | FB-OH1-875 | Complex C (OH1-B3, Layer XVg) | Compound C7, Fosa 3, before platform (**Level 2a**) | 74.2 | −22.9 | 2487 +- 22 | 756-734 BC 10.5% | **771-539 BC** 95.4% | | |
| | | | | | | | 696-680 BC 7.8% | | | |
| | | | | | | | 671-664 BC 3.3% | | | |
| | | | | | | | 649-606 BC 21.3% | | | |
| | | | | | | | **596-546 BC** 25.4% | | | |
| AA112582 | FB-OH1-865 | Complex C (OH1-A0, Layer XIc) | Compound C7, Fosa 2 associated with platform (**Level 2e**) | 64.2 | −24.2 | 2490 +- 22 | 756-740 BC 8.7% | **771-541 BC** 95.4% | | |
| | | | | | | | 693-680 BC 7.3% | | | |
| | | | | | | | 671-665 BC 3.1% | | | |
| | | | | | | | 648-606 BC 22.7% | | | |
| | | | | | | | **597-548 BC** 26.5% | | | |
| AA112583 | FB-OH1-559 | Complex C (OH1-B1, Layer VII) | Compound C7, floor that covers platform (**Level 2d**) | 63.1 | −21.8 | 2457 +- 21 | **748-688 BC** 31.0% | 754-682 BC 33.1% | | |
| | | | | | | | 666-642 BC 11.2% | 670-609 BC 17.4% | | |
| | | | | | | | 567-513 BC 21.1% | **594-456 BC** 40.3% | | |
| | | | | | | | 501-485 BC 4.9% | 444-417 BC 4.5% | | |
| AA112584[*1] | FB-OH1-830 | Complex C (OH1-B1, Layer XIIa) | Compound C7, before platform, after Fosa 3 | 20.6 | −24.1 | 2374 ± 21 | 466-436 BC 25.6% | **516-393 BC** 95.4% | | |
| | | | | | | | **422-397 BC** 42.7% | | | |

_Texoloc Phase (Tres Marias Complex)_

| | | | | | | | | | | |
|---|---|---|---|---|---|---|---|---|---|---|
| AA109304 | FF-P1-41 | Complex TM (Pozo 1, Layer IIIc) | Within earthern floor under Str. TM10a (**Level 8**) | 75 | −24.0 | 2483 ± 20 | 754-731 BC 11.5% | **768-539 BC** 95.4% | | |
| | | | | | | | 700-681 BC 9.0% | | | |
| | | | | | | | 669-664 BC 2.6% | | | |
| | | | | | | | 651-609 BC 20.1% | | | |

(_Continued_)

**Table 1.** (*Continued*)

| Lab# | Sample ID | Provenience | Context | %C | $\delta^{13}C$ (‰) | $^{14}C$ age BP | Calibrated calendar yrs (1 sigma) | P | Calibrated calendar yrs (2 sigma) | P |
|---|---|---|---|---|---|---|---|---|---|---|
| AA109305 | FF-P1-58 | Complex TM (Pozo 1, Layer Ivc) | Trash pit (Fosa 1) under Str. TM10a (**Level 7**) | 62 | −24.4 | 2476 ± 20 | **594-545 BC** 25.0%<br>751-720 BC 16.7%<br>708-684 BC 12.5%<br>668-663 BC 2.1%<br>653-634 BC 9.7%<br>621-614 BC 3.1%<br>**591-544 BC** 24.1% | | **766-515 BC** | 95.4% |
| AA109306 | FF-P1-77 | Complex TM (Pozo 1, Layer VI) | Pit feature (Fosa 3) under Str. TM10a (**Level 6**) | 70 | −25.0 | 2478 ± 20 | 752-722 BC 15.7%<br>707-684 BC 12.0%<br>668-664 BC 2.2%<br>652-633 BC 9.9%<br>622-613 BC 3.9%<br>**591-545 BC** 24.5% | | **767-516 BC** | 95.4% |
| AA109307 | FF-P1-160 | Complex TM (Pozo 1, Layer X) | Burial F1 under Str. TM10a (**Level 4**) | 66 | −9.2 | 2476 ± 20 | 751-720 BC 16.7%<br>708-684 BC 12.5%<br>668-663 BC 2.1%<br>653-634 BC 9.7%<br>621-614 BC 3.1%<br>**591-544 BC** 24.1% | | **766-515 BC** | 95.4% |
| AA109309 | FF-P2-70 | Complex TM (Pozo 2, Layer Vb) | Trash midden (Level 5-6 or earlier) | 68 | −24.4 | 2540 ± 22 | **788-753 BC** 41.9%<br>682-669 BC 12.4%<br>610-593 BC 14.0% | | **794-747 BC**<br>689-665 BC<br>643-563 BC | 44.6%<br>15.2%<br>35.6% |
| AA109310 | FF-P2-89 | Complex TM (Pozo 2, Layer VIb) | Trash midden (**Level 1-2**) | 66 | −23.3 | 2479 ± 20 | 752-725 BC 14.8%<br>706-684 BC 11.9%<br>668-664 BC 2.1%<br>651-633 BC 9.9%<br>622-613 BC 4.4%<br>**591-545 BC** 25.2% | | **768-517 BC** | 95.4% |
| AA109311 | FF-P5-31 | Complex TM (Pozo 5, Layer VIII) | Bell-shaped pit (Level 6-7 or earlier) | 63 | −23.4 | 2469 ± 20 | **750-685 BC** 34.3%<br>667-636 BC 14.3% | | **760-477 BC** | 95.4% |

| Lab ID | Sample | Complex | Feature | n | δ13C | ¹⁴C age BP | Cal 1σ | % | Cal 2σ | % |
|---|---|---|---|---|---|---|---|---|---|---|
| | | | | | | | 589-541 BC | 19.7% | | |
| AA109312 | FF-P5-83 | Complex TM (Pozo 5, Layer X) | Bell-shaped pit (Level 6-7 or earlier) | 65 | −23.7 | 2467 ± 21 | **750-685 BC** | 34.6% | 758-678 BC | 36.4% |
| | | | | | | | 667-636 BC | 14.3% | **672-476 BC** | 58.5% |
| | | | | | | | 589-578 BC | 3.8% | 431-426 BC | 0.5% |
| | | | | | | | 573-539 BC | 15.5% | | |
| AA109313 | FF-P8-27 | Complex TM (Pozo 8, Layer IIIb) | Earthen floor of patio at Compound TM10 (**Level 9**) | 67 | −25.9 | 2432 ± 20 | 717-711 BC | 3.3% | 744-691 BC | 15.2% |
| | | | | | | | 659-655 BC | 2.0% | 665-646 BC | 6.6% |
| | | | | | | | **542-460 BC** | 51.4% | **550-408 BC** | 73.6% |
| | | | | | | | 439-420 BC | 11.5% | | |
| AA109314*² | FF-P9-28 | Complex TM (Pozo 9, Layer VIIIb) | Fill of pit feature in front of Str. TM10c (Level 9) | 60 | −24.8 | 2659 ± 20 | **824-802 BC** | 68.3% | 892-880 BC | 5.3% |
| | | | | | | | | | **833-795 BC** | 90.2% |
| AA109315 | FF-P7-36 | Complex TM (Pozo 7, Layer IVb) | Pit feature (Fosa 2) in residential area | 66 | −24.6 | 2479 ± 20 | 752-725 BC | 14.8% | **768-517 BC** | 95.4% |
| | | | | | | | 706-684 BC | 11.9% | | |
| | | | | | | | 668-664 BC | 2.1% | | |
| | | | | | | | 651-633 BC | 9.9% | | |
| | | | | | | | 622-613 BC | 4.4% | | |
| | | | | | | | **591-545 BC** | 25.2% | | |
| AA109320 | FF-P6-83 | Complex TM (Pozo 6, Layer VIIa) | Pit feature in open space | 65 | −24.0 | 2522 ± 21 | 775-750 BC | 20.7% | 781-742 BC | 25.6% |
| | | | | | | | 685-667 BC | 13.8% | 693-663 BC | 18.2% |
| | | | | | | | **636-589 BC** | 31.0% | **647-548 BC** | 51.7% |
| | | | | | | | 578-573 BC | 2.7% | | |
| AA110707 | FF-P7-21 | Complex TM (Pozo 7, Layer III) | Hearth 1 | 57 | −25.3 | 2481 ± 20 | 753-726 BC | 14.0% | **766-539 BC** | 94.7% |
| | | | | | | | 701-683 BC | 9.5% | 527-521 BC | 0.8% |
| | | | | | | | 669-664 BC | 2.5% | | |
| | | | | | | | 651-631 BC | 10.3% | | |
| | | | | | | | 625-611 BC | 6.6% | | |
| | | | | | | | **593-545 BC** | 25.3% | | |

### Early Tezoquipan Phase

| Lab ID | Sample | Complex | Feature | n | δ13C | ¹⁴C age BP | Cal 1σ | % | Cal 2σ | % |
|---|---|---|---|---|---|---|---|---|---|---|
| AA105263 | R1-V9 | Salvage excavation (Pozo 1, Layer VII) | Ceremonial cache | N/A | −25.5 | 2168 ± 30 | **351-290 BC** | 37.6% | 359-276 BC | 42.7% |
| | | | | | | | 209-164 BC | 30.7% | 261-244 BC | 2.6% |
| | | | | | | | | | **235-103 BC** | 50.2% |
| AA110693 | FB-C2O-504 | Complex C (Cala 2O, floor) | Earthern floor in front of Str. C5-Sub1 | 65 | −24.2 | 2249 ± 19 | 382-356 BC | 26.2% | 389-350 BC | 32.5% |
| | | | | | | | **280-232 BC** | 42.1% | **303-208 BC** | 62.9% |
| AA110704 | FB-C3J-518 | Complex C (Cala 3J, Layer XVb) | Pit feature associated with Str. C5-Sub1 | 56 | −25.3 | 2267 ± 19 | **390-359 BC** | 44.8% | **395-352 BC** | 51.4% |
| | | | | | | | 276-261 BC | 13.8% | 288-227 BC | 42.3% |
| | | | | | | | 244-234 BC | 9.7% | 219-210 BC | 1.7% |

Note: calibration was conducted using OxCal 4.4/IntCal20 atmosphere.
*¹These samples were excluded from the analysis due to possible contamination or intrusion from younger contexts.
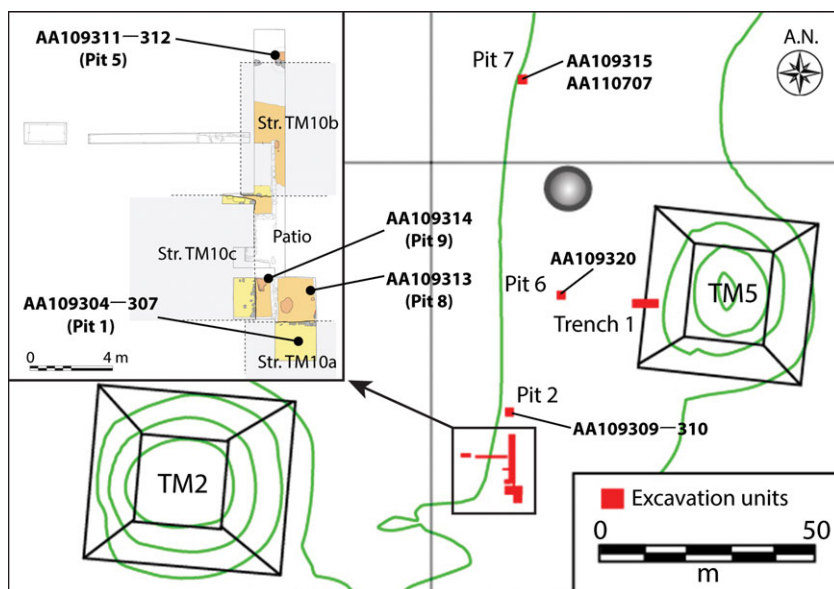*²This sample likely represents old wood and thus was excluded from the analysis.

**Figure 4.** *Map of Tres Marias Complex showing the location of excavation units and the provenience of radiocarbon samples. The inserted map shows Compound TM10.*

whose provenience was already discussed above. The third sample (AA-105263) came from a ceremonial cache that was found during survey in the southwestern sector of the site and excavated as a salvage operation.

### Excavations and samples at the Tres Marias Complex (Complex TM)

The Tres Marias Complex is located several hundred meters east of Complex C. It features Terminal Formative pyramids, platforms, and plazas visible on the surface (Figure 4). Below these civic-ceremonial structures, our test excavations revealed a residential compound (Compound TM10), additional domestic features (e.g., trash pits), and at least nine superposed occupation levels from the Texoloc phase (Murakami et al. 2017b). We identified and defined the earliest eight occupation levels from the stratigraphy of superposed pit features in Test Pit 1 (*Pozo 1*). Compound TM10 represented the ninth level; it consisted of three low, masonry platforms (Structures TM10a–c) arranged around a central patio (Figure 4). The depth of Texoloc deposits at Compound TM10 differed from those at Compound C7. The superposed floors from Compound C7 were closely deposited, amounting to a thickness of 10–30 cm across the excavated area. In contrast, roughly 20 cm separated each occupation level below Compound TM10, resulting in Texoloc-phase deposits in Test Pit 1 that spanned 2 meters of depth. Test Pits 2, 5, 8, and 9 had Middle Formative layers that could be roughly correlated with the stratigraphy in Test Pit 1 (Table 1). Middle Formative deposits in Test Pits 6 and 7 were too shallow to be securely associated with the stratigraphy in the other test pits.

We collected a total of 13 samples (all wood charcoal) from Texoloc contexts at the Tres Marias Complex (one of these samples was excluded from the analysis for reasons described below). We assigned six samples to specific occupational levels as defined in Test Pit 1 (Table 1): Sample AA-109310 to Levels 1–2; Sample AA-109307 to Level 4; Sample AA-109306 to Level 6; Sample AA-109305 to Level 7; Sample AA-109304 to Level 8; and Sample AA-109313 to Level 9. Four of these samples came from Test Pit 1 while two came from other test pits. Although Test Pits 1 and 2 were spaced 20 meters apart and their stratigraphy correlated poorly, we felt comfortable tentatively assigning Sample AA-109310 from Test Pit 2 to Levels 1–2 because the sample came from a midden directly

above the sterile layer, roughly 1.5 m below the depth of the sterile layer in Test Pit 1 (see Supplementary Materials for stratigraphic profiles). We did not encounter secure contexts associated with Levels 3 and 6 from which to collect samples. Sample AA-109314 was collected from Test Pit 9 and yielded a conspicuously old date (see below), so we excluded it from further analysis. We could not securely assign the other samples to specific occupation levels, but we suggest possibilities in Table 1.

### Charcoal Outlier Model

All samples were wood charcoal and could, therefore, pose the old wood problem: a major temporal discrepancy between the feature/primary context and the date the original wood, from which the charcoal stemmed, was cut. Identifying the species of tree can help isolate the effect of old wood, especially in the case of short-lived species (e.g., Tsukamoto et al. 2020). We did not undertake this type of analysis for this paper, but instead used Bayesian statistics to gauge the probability of old wood inclusions among our Texoloc samples. We did so by creating charcoal outlier models with a Bayesian statistical method featured in OxCal version 4.4 following Bronk Ramsey (2009a; see also Christen 1994) (see Figures S7 and S8 in Supplementary Materials for reports). For Charcoal Model 1, we set the prior probability of outliers at 5% (following Bronk Ramsey 2009a:1026) and grouped all Texoloc samples as a single phase. Three samples (AA-110704, AA-109314, and AA-112584) were highlighted as outliers given posterior probabilities of 75%, 61%, and 31%, respectively. For comparison, all other samples had posterior probabilities ranging from 3–5%. The agreement indices (see Results below) of these samples were also quite low (38%, 48%, and 35%, respectively). For Charcoal Model 2, we omitted these Texoloc samples (AA-110704 was grouped with the Tezoquipan samples as mentioned above) and added Tlatempa and Tezoquipan samples to constrain the range of Texoloc dates. This iteration did not highlight any outliers as potential old wood inclusions (see Supplementary Materials), so we proceeded to further Bayesian modeling with this set of samples.

### Simulation

To determine whether building reliable chronological models was possible in the middle of the Hallstatt Plateau, we conducted simulations using predetermined dates with specific intervals in OxCal 4.4 with the IntCal 20 calibration curve (Bronk Ramsey 1995; 2009b; 2017; Buck 2001; Reimer et al. 2013, 2020). Simulations are a powerful tool to explore the range of accuracy we should expect in our chronological modeling (e.g., Krus and Cobb 2018; McDonald and Manning 2023). We experimented with three sets of intervals between 650 BC and 500 BC, the proposed range for the Texoloc phase: (1) 30-year intervals with six dates; (2) 15-year intervals with 11 dates; and (3) 10-year intervals with 16 dates (a standard deviation of 20 years was added to all dates; see Table 2 for a summary and Figures S9-S14 in Supplementary Materials for details). We ran separate simulations with Sequence and Phase functions for both the start and end boundaries of the phase. The results show that the 650 BC start date and 500 BC end date for the Texoloc phase are within the 68.3% probability range of all models except for one (start boundary based on phase method with 10-year intervals and 16 samples). The phase function simulations seemed to provide less reliable outcomes given that the start and end date ranges were in the order of 200-300 years at 68.3% probability. Simulations built with sequence functions consistently produced better models as their means and medians were closer to the phase dates we were corroborating. The sequence method model with 10-year intervals and 16 samples yielded means and medians within 5 years of the 650 BC start date and within 2 years of the 500 BC end date of the phase (Table 2). This suggests to us that reliable chronologies can be built using stratigraphically sequenced dates. We expect that model building will improve substantially when constraining the possible ranges by adding samples/dates that preceded and followed the Texoloc phase.

**Table 2.** *Results of simulations (separate modes and their probable ranges for both 1σ and 2σ probabilities were lumped together as a single range for each model)*

|  | 1 σ cal BC | Range | 2 σ cal BC | Range | Mean | Median |
|---|---|---|---|---|---|---|
| **Start Boundary (set at 650 BC)** | | | | | | |
| *Sequence method* | | | | | | |
| 30-year intervals (6 samples) | 756-562 BC | 194 | 877-548 BC | 329 | 683 BC | 663 BC |
| 15-year intervals (11 samples) | 758-550 BC | 208 | 771-546 BC | 225 | 658 BC | 659 BC |
| 10-year intervals (16 samples) | 693-611 BC | 82 | 773-581 BC | 192 | 655 BC | 645 BC |
| *Phase method* | | | | | | |
| 30-year intervals (6 samples) | 785-560 BC | 225 | 883-543 BC | 340 | 710 BC | 718 BC |
| 15-year intervals (11 samples) | 763-551 BC | 212 | 784-544 BC | 240 | 676 BC | 699 BC |
| 10-year intervals (16 samples) | 777-701 BC | 76 | 798-557 BC | 241 | 719 BC | 732 BC |
| **End Boundary (set at 500 BC)** | | | | | | |
| *Sequence method* | | | | | | |
| 30-year intervals (6 samples) | 531-406 BC | 125 | 728-249 BC | 479 | 447 BC | 456 BC |
| 15-year intervals (11 samples) | 718-454 BC | 264 | 735-384 BC | 351 | 520 BC | 505 BC |
| 10-year intervals (16 samples) | 533-481 BC | 52 | 658-422 BC | 236 | 498 BC | 502 BC |
| *Phase method* | | | | | | |
| 30-year intervals (6 samples) | 702-396 BC | 306 | 733-300 BC | 433 | 501 BC | 489 BC |
| 15-year intervals (11 samples) | 715-434 BC | 281 | 731-371 BC | 360 | 538 BC | 506 BC |
| 10-year intervals (16 samples) | 686-500 BC | 186 | 731-461 BC | 270 | 596 BC | 614 BC |

### Bayesian modeling

We produced nine primary models (and nine variants) of the consecutive Tlatempa, Texoloc and Tezoquipan phases to define the beginning, end, and duration of the Texoloc phase (Table 3; see Supplementary Materials for output plots). We used OxCal version 4.4 with the IntCal 20 calibration curve and different combinations of Texoloc samples from the 26 described above; the same combination of Tlatempa and Tezoquipan phase samples was used throughout (note that the Tezoquipan samples were always put in a Phase function, which was not always shown in the figures in the interest of space). We used five different methods based on the Phase and Sequence functions (e.g., Bronk Ramsey 1995, 2009b, 2017; Buck et al. 1992; Steier and Rom 2000) to build the models: (1) sequencing Phase functions (Models 1-3); (2) sequencing samples (Models 4-5); (3) sequencing Sequence functions (Models 6-7); (4) sequencing overlapping Sequence functions (Model 8); and (5) cross referencing sequences from the two architectural complexes within the Sequence function (Model 9) (Table 3). We included the Interval function in Models 1–3 to estimate the duration of the Texoloc phase.

The different combinations of Texoloc samples included: all samples in Model 1; samples solely from Complex C in Models 2, 4, and 6; and samples solely from the Tres Marias Complex in Models 3, 5, and 7. Only chronologically well-defined samples from the complexes were used in Models 4-7; these sets of samples from both complexes were combined in Models 8 and 9. We placed a single boundary query between functions to model the Tlatempa, Texoloc and Tezoquipan phases as contiguous (Bronk Ramsey 2009b) and obtain probability distributions for their transition dates.

We constructed nine variant models with the same sets of samples described above that did not impose contiguous archaeological phases on the modeling. Models 4NB ("No Boundary") and 5NB, for example, contained no boundary queries. Instead we considered the phase transition date to fall between the youngest Tlatempa sample and the oldest Texoloc sample. For the other variant models (denominated with "S" after model number), we inserted two boundary queries between phases to create "Sequential Models" (Bronk Ramsey 2009b), which allowed for time lapses between phases (sequential

**Table 3.** *Summary of Bayesian models*

| | Method | Texoloc samples included in the model | Notes |
|---|---|---|---|
| Model 1 | Phase | 7 samples from Complex C and 12 samples from Complex Tres Marias | |
| Model 2 | Phase | 7 samples from Complex C | |
| Model 3 | Phase | 12 samples from Complex Tres Marias | |
| Model 4 | Sequence | 7 samples (Levels 2a-e) from Complex C | Levels 2a and 2e consist of two samples each that were grouped under the phase function. |
| Model 5 | Sequence | 6 samples from Complex Tres Marias | Samples from Levels 5-7 were put together in a phase block. |
| Model 6 | Phase/Sequence | 7 samples from Complex C | Levels 2a and 2e consist of two samples each that were grouped under the phase function. |
| Model 7 | Phase/Sequence | 6 samples from Complex Tres Marias | Samples from Levels 5-7 were put together in a phase block. |
| Model 8 | Overlapping Sequence | 7 samples from Complex C and 6 samples from Complex Tres Marias | Sequences from both Complexes C and TM were contained as overlapping sequences within the Texoloc phase block. |
| Model 9 | Cross Referencing | 7 samples from Complex C and 6 samples from Complex Tres Marias | Start of Complex C was cross referenced to the start of Complex Tres Marias. |

models are presented in Supplementary Materials). Opting for either contiguous or sequential models essentially depends on how we conceptualize phase transitions in ancient societies. For the case of Tlalancaleca, we base this decision on careful observation of the stratigraphy. At Complexes C and Tres Marias, the phases correspond well with the architectural sequences described above. Importantly, we did not observe any substantial layer or deposit that would indicate a long-time lapse between phases and the changing material culture recovered from excavations. That said, we recognize the difficulty of discerning subtle gaps in time on the scale of years or decades. To narrow down the date range of phase transitions, we cross-validated results across models. We report marginal posterior distributions and ranges at 68.3% and 95.4% of modeled results (Tables 4 and 5); we refer to 68.3% ranges in text first and 95.4% ranges in parenthesis to facilitate reading results (see also the results of simulations above). Probabilities at 95.4% are often split into different segments of the curve over ranges of ∼150 years and the presentation of such segments could have complicated our discussion of the Texoloc phase with its estimated duration of 150 years.

The methods and models exhibited different strengths and weaknesses. Model 1 (Phase method), for example, included the greatest number of samples yet the Phase functions did not draw on the subtle stratigraphic information between them (also the case in Models 2 and 3). Models 4–9 considered the stratigraphic order of samples yet Models 4 and 5 (Sequence method) did not consider their archaeological phase assignations. As a result, phase transition dates were based more on individual samples than sets of samples. Models 6 and 7 (Phase/Sequence method) took samples' stratigraphic order and archaeological phase assignations into account but relied on fewer samples to do so. Models 8

**Table 4.** *Date ranges for the Tlatempa-Texoloc boundaries (more likely 1σ and 2σ date ranges are in bold)*

| | 1 σ cal BC | P | Mode* | 2 σ cal BC | P | Mode* | Mean | Median |
|---|---|---|---|---|---|---|---|---|
| *Phase method* | | | | | | | | |
| Model 1 (all samples) | **723-640 BC** | 68.3% | 695 (650) BC | **734-613 BC** | 83.0% | 695 (650) BC | 668 BC | 675 BC |
| | | | | 606-561 BC | 12.5% | 585 BC | | |
| Model 2 (Complex C) | **720-674BC** | 42.5% | 690 BC | **736-587 BC** | 95.4% | 690 (645) BC | 664 BC | 673 BC |
| | 662-632 BC | 25.8% | 645 BC | | | | | |
| Model 3 (Complex TM) | **725-637 BC** | 68.3% | 695 (650) BC | **734-561 BC** | 95.4% | 695 (650) BC | 664 BC | 673 BC |
| *Sequence method* | | | | | | | | |
| Model 4 (Complex C) | 726-681 BC | 39.4% | 695 BC | **741-614 BC** | 91.0% | 655 (695) BC | 672 BC | 676 BC |
| | **666-641 BC** | 28.9% | 655 BC | 594-576 BC | 2.9% | 585 BC | | |
| | | | | 571-560 BC | 1.6% | 560 BC | | |
| Model 5 (Complex TM) | 717-681 BC | 24.3% | 695 BC | **732-547 BC** | 95.4% | 645 (695) BC | 643 BC | 647 BC |
| | **661-626 BC** | 24.8% | 645 BC | | | | | |
| | 585-549 BC | 19.1% | 560 BC | | | | | |
| *Phase/Sequence method* | | | | | | | | |
| Model 6 (Complex C) | **731-682 BC** | 57.6% | 695(720) BC | **742-637 BC** | 95.4% | 695 (720) BC | 691 BC | 696 BC |
| | 663-651 BC | 10.7% | 655 BC | | | | | |
| Model 7 (Complex TM) | 724-676 BC | 33.0% | 695 BC | **732-560 BC** | 95.4% | 645 (695) BC | 654 BC | 653 BC |
| | **664-617 BC** | 35.3% | 645 BC | | | | | |
| *Overlapping Sequence method* | | | | | | | | |
| Model 8 (both complexes) | **731-626 BC** | 68.3% | 690 (650) BC | **734-560 BC** | 95.4% | 690 (650) BC | 660 BC | 670 BC |
| *Cross Referencing method* | | | | | | | | |
| Model 9 (both complexes) | 708-682 BC | 17.7% | 695 BC | **726-549 BC** | 95.4% | 560 (645) BC | 633 BC | 644 BC |
| | 661-639 BC | 19.0% | 645 BC | | | | | |
| | **591-551 BC** | 31.6% | 560 BC | | | | | |

*The date within parenthesis shows the secondary mode when present.

**Table 5.** *Date ranges for the Texoloc-Tezoquipan boundaries (more likely 1σ and 2σ date ranges are in bold)*

| | 1 σ cal BC | P | Mode* | 2 σ cal BC | P | Mode* | Mean | Median |
|---|---|---|---|---|---|---|---|---|
| *Phase method* | | | | | | | | |
| Model 1 (all samples) | 622-606 BC | 6.6% | 615 BC | 682-678 BC | 0.4% | 680 BC | 560 BC | 549 BC |
| | **575-508 BC** | 61.7% | 540 BC | 659-654 BC | 0.5% | 656 BC | | |
| | | | | **648-480 BC** | 94.5% | 540 BC | | |
| Model 2 (Complex C) | 616-604 BC | 3.1% | 610 BC | **652-366 BC** | 95.4% | 540 BC | 514 BC | 522 BC |
| | **592-448 BC** | 65.1% | 540 BC | | | | | |
| Model 3 (Complex TM) | 638-626 BC | 4.2% | 630 BC | 688-672 BC | 1.7% | 680 BC | 550 BC | 545 BC |
| | 615-610 BC | 2.0% | 610 BC | **667-447 BC** | 93.8% | 540 BC | | |
| | **580-496 BC** | 62.1% | 540 BC | | | | | |
| *Sequence method* | | | | | | | | |
| Model 4 (Complex C) | **625-532 BC** | 68.3% | 550 BC | 688-659 BC | 3.2% | 680 BC | 565 BC | 569 BC |
| | | | | **646-438 BC** | 92.30% | 550 BC | | |
| Model 5 (Complex TM) | **551-448 BC** | 68.3% | 540 BC | 698-687 BC | 0.8% | 692 BC | 496 BC | 507 BC |
| | | | | 659-638 BC | 1.8% | 645 BC | | |
| | | | | **566-362 BC** | 92.9% | 540 BC | | |
| *Phase/Sequence method* | | | | | | | | |
| Model 6 (Complex C) | **591-456 BC** | 60.2% | 540 BC | **632-357 BC** | 95.4% | 540(385) BC | 494 BC | 507 BC |
| | 403-380 BC | 8.1% | 385 BC | | | | | |
| Model 7 (Complex TM) | **543-451 BC** | 52.4% | 535 BC | 654-642 BC | 0.6% | 648 BC | 464 BC | 469 BC |
| | 415-382 BC | 15.9% | 390 BC | **566-329 BC** | 94.9% | 535(390) BC | | |
| *Overlapping Sequence method* | | | | | | | | |
| Model 8 (both complexes) | **554-460 BC** | 42.5% | 535 BC | 687-681 BC | 0.4% | 685 BC | 468 BC | 472 BC |
| | 434-373 BC | 25.8% | 385 BC | 647-595 BC | 4.6% | 635 BC | | |
| | | | | **586-317 BC** | 90.2% | 535(385) BC | | |
| | | | | 309-305 BC | 0.2% | —— | | |
| *Cross Referencing method* | | | | | | | | |
| Model 9 (both complexes) | 694-681 BC | 3.9% | 690 BC | **698-359 BC** | 95.4% | 555(640) BC | 532 BC | 547 BC |
| | 650-626 BC | 11.3% | 640 BC | | | | | |
| | **588-479 BC** | 45.9% | 555 BC | | | | | |
| | 409-377 BC | 7.2% | 385 BC | | | | | |

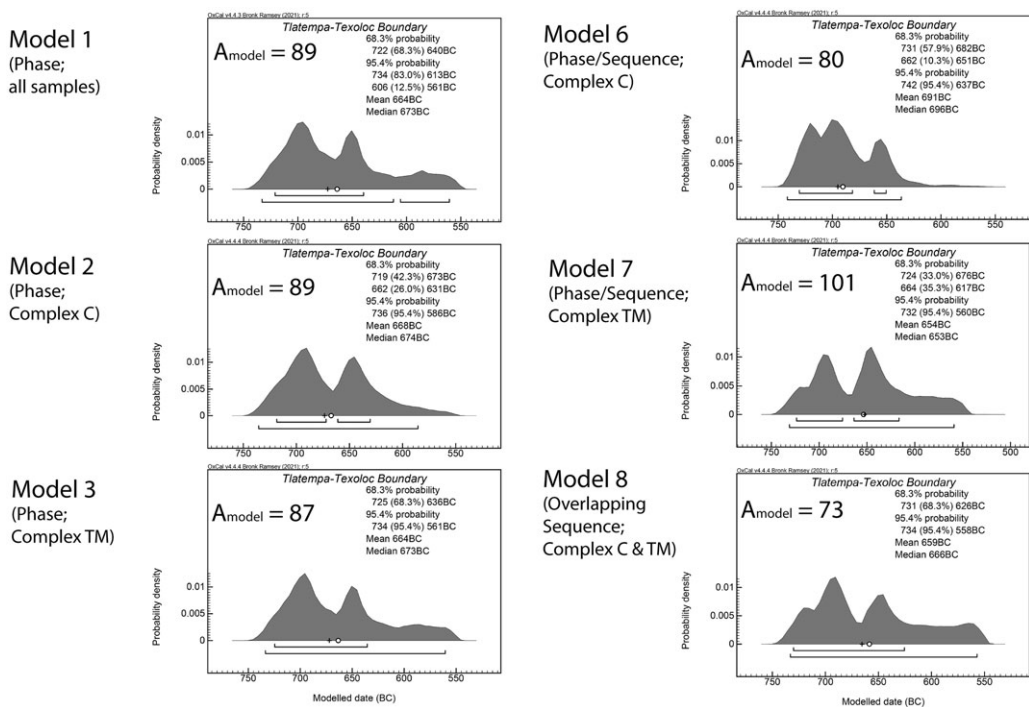*The date within parenthesis shows the secondary mode when present.

**Figure 5.** *Tlatempa-Texoloc boundaries for contiguous models. Horizontal bars under the distributions are at 1σ and 2σ probability ranges.*

and 9 accounted for samples' stratigraphic order, phase assignations, and combined Texoloc samples from Complexes C and Tres Marias, resulting in models with the second largest sample size. In Model 8 (Overlapping Sequence method), however, we could not control the amount of overlap between the two separate sequences. Model 9 (Cross Referencing method) required that we assume the start or end date (or both) of the separate sequences were contemporaneous even though they were not. The analytical strength of these models, therefore, comes from considering them collectively. We identify patterns that persist across the different models and consider them a solid basis for chronology building.

## Results and discussion

All contiguous Bayesian models, except for Model 9, illustrate a bimodal probability distribution for the Tlatempa-Texoloc transition with modes around 695 and 650 cal BC (Table 4; Figure 5); means varied from 691 to 633 cal BC and medians from 696 to 644 cal BC. Models 1–3, 6, and 8 point to the earlier mode while Models 4, 5, and 7 point to the later mode (Figure 5; see Supplementary Materials for modeled dates). To put it differently, the Phase method points to 695 cal BC while models that stratigraphically sequenced samples point to 650 cal BC. Additionally, models based on samples from Complex C tend to favor 695 cal BC, while models based on samples from the Tres Marias Complex point to both modes (we will come back to this point below). In each case, it seems the oldest Texoloc sample affected the modeling. For example, the most probable date range of the oldest Texoloc sample (AA-110702) from Complex C was 665-643 cal BC (43.9%) in Model 6 (670-612 cal BC [57.2%] for 2σ). This range was much narrower than the range of the oldest Texoloc sample (AA-109310) from the Tres Marias Complex, which was 671–608 cal BC (46.1%) in Model 7 (708–550 cal BC [95.4%] for 2σ). The narrower date range of Sample AA-110702 around 650 cal BC likely pushed the Tlatempa-Texoloc transition to an earlier range and its most probable mode to 695 cal BC in the Complex
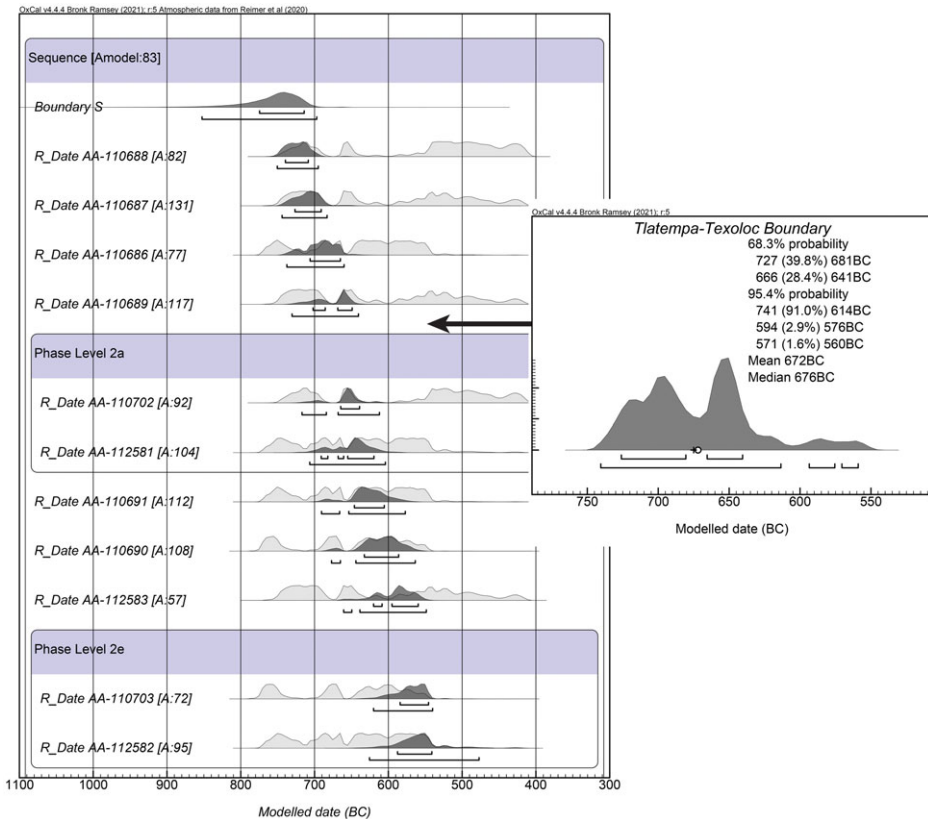
**Figure 6.** *Model 4NB (Sequence method at Complex C without boundary) with an insertion of the Tlatempa-Texoloc boundary from Model 4 (Sequence method at Complex C). Horizontal bars under the distributions are at 1σ and 2σ probability ranges.*

C models. We favor 650 cal BC for the Tlatempa-Texoloc boundary because the oldest Texoloc samples at Complex C calibrated to around 650 cal BC in Models 4, 6, 8 and 9. It is equally worth noting that the most probable range of the youngest Tlatempa sample (AA-110689) in Model 4NB was 669-650 cal BC (47.6%) (731–641 cal BC [95.4%] for 2σ; result consistent in Model 5NB which used Tres Marias samples) (Figure 6). This suggests 695 cal BC is too early a boundary date between the Tlatempa and Texoloc phases. While there are critiques on the use of a mode (or intercept) for calibrating individual dates (Telford et al. 2004; see also Michczyńska and Michczyńska 2006), the posterior probability distribution of the boundary function is not a simple reflection of the calibration curve but its interaction with multiple dates (or sets of dates) (Bronk Ramsey 2009b). Modes of boundary functions, therefore, are model-specific and we believe this makes them a reliable statistic. The average of means for the Tlatempa-Texoloc boundaries from Models 1–9 was 661±17 cal BC, supporting further a 650 cal BC transition date. We discuss additional reasons for supporting 650 cal BC as the Tlatempa-Texoloc transition date below.

Contiguous models built with different methods and samples consistently pointed to a Texoloc-Early Tezoquipan transition around 540 cal BC, with modes as early as 555 cal BC and as late as 535 cal BC depending on the model (Table 5; the mean ranges from 565 to 464 cal BC and the median from 569 to 469 cal BC). The youngest Texoloc sample from the Tres Marias Complex suggested a Texoloc-Tezoquipan transition date around 545 cal BC. This charcoal was incrusted in a floor matrix, however, so it likely represents the date of the last construction episode and, conceivably, human activities persisted on this occupation level for several more decades. Given these data and line of reasoning, we

place the Texoloc-Tezoquipan transition around 500 cal BC. The average of means for this transition (boundary) in Models 1–9 was 516±38 cal BC, thus consistent with the modes.

In Models 1–3, we estimated the duration of the Texoloc phase using the Interval function, which provides a probability distribution for its duration. In keeping with our treatment of radiocarbon dates, we consider phase duration ranges at 68.3% of the probability density functions. Results were highly consistent across the models. In Model 1, the most probable Texoloc phase duration was 65–169 years (56.3%) with a mode at 120 years, the mean at 105 years, and the median at 107 years (0–200 years [95.4%] for 2σ). In Model 2, the most probable duration was 47–227 years (68.3%) with a mode at 120 years, the mean at 154 years, and the median at 146 years (0-311 years [95.4%] for 2σ). In Model 3, the most probable duration was 45–176 years (59.3%) with the mode landing at 115 years, the mean at 114 years, and the median at 111 years (0–240 years [95.4%] for 2σ). These estimates were based strictly on radiocarbon samples and dates; the context of samples and their implications for human occupation were not considered. These estimated durations, therefore, are likely underestimates, with the actual duration of the Texoloc phase several decades longer. The estimated duration of the Texoloc phase can be considered with the Texoloc-Tezoquipan boundary produced by the models as an additional method for estimating the start date of the Texoloc phase. In other words, counting back 120 years from 540 cal BC (mode for Texoloc-Tezoquipan boundary across models) leads to an estimated start date of 660 cal BC for the Texoloc phase. This lends further support for favoring the mode at 650 cal BC as the Tlatempa-Texoloc transition.

We use agreement indices to scan for problematic samples and discrepancies between model and data in evaluating these results (Bronk Ramsey 2009b, 354). Sample agreement indices represent the overlap between the distributions of unmodeled and modeled calibrated dates (i.e., overlap between the original and marginal posterior distribution) (Bayliss 2007; Bronk Ramsey 1995, 2009b). A high agreement index *does not* equate to a "better" or "more probable" model, as Bayliss (2007, 81) and Hamilton and Krus (2018, 192) note, but rather consistency between the data (i.e., measured isotope ratio of radiocarbon), probabilities, and model (e.g., stratigraphic order) (Bronk Ramsey 1995, 2009b). Thus, low agreement indices can signal sample intrusions, errors in measurement, or incorrect/unlikely parameters and priors (Bronk Ramsey 2009b, 356). An agreement index of 60% is the commonly used threshold for considering samples as problematic (Bronk Ramsey 1995, 2009b). We use this threshold in evaluating results here, but not without critical evaluation.

Overall agreement indices range from 73% (Model 9) to 108% (Model 5NB) and model agreement indices range from 65% (Model 9) to as high as 108% (Model 5NB), suggesting no salient inconsistencies between data and models. Importantly, agreement indices for individual samples are high across models and methods. Agreement indices near the 60% threshold for Samples AA-109309 (Models 1 and 3), AA-109313 (Model 1), and Sample AA-112583 (Model 6). There are only three instances in which the sample agreement index drops below 60%: Sample AA-110686 at 58% in Model 6 and Sample AA-110702 at 51% in Model 8 and 46% in Model 9. We retained Samples AA-110686 and AA-110702 in our models because they were not consistently problematic across iterations. Thus, agreement indices overwhelmingly suggest no problematic discrepancies, confirming all models as "valid interpretations of the evidence" (Bayliss 2007, 81).

Despite all being "valid" interpretations, we find certain models more compelling, and patterns emerge consistently across them. It seems clear that the sequence from Complex C started earlier than the sequence from the Tres Marias Complex. We observe this when comparing the models that separated the samples from each complex (i.e. Models 4 vs. 5; Models 6 vs. 7; Table 4). In Model 8 (Figure 7), the sequences from the two architectural complexes were treated as overlapping within a single phase and the pattern holds: the Complex C sequence started earlier (Figures 7 and 8). This observation can account for the poor fit between Model 9 and the data as the start date was cross referenced between the two complexes (we also created a model to cross reference the end date, but its model agreement index was below 60% and so it was not presented in this paper).

It is equally clear that the sequence from the Tres Marias Complex endured longer than the sequence from Complex C. The youngest sample from the Tres Marias Complex seems to be on the final segment
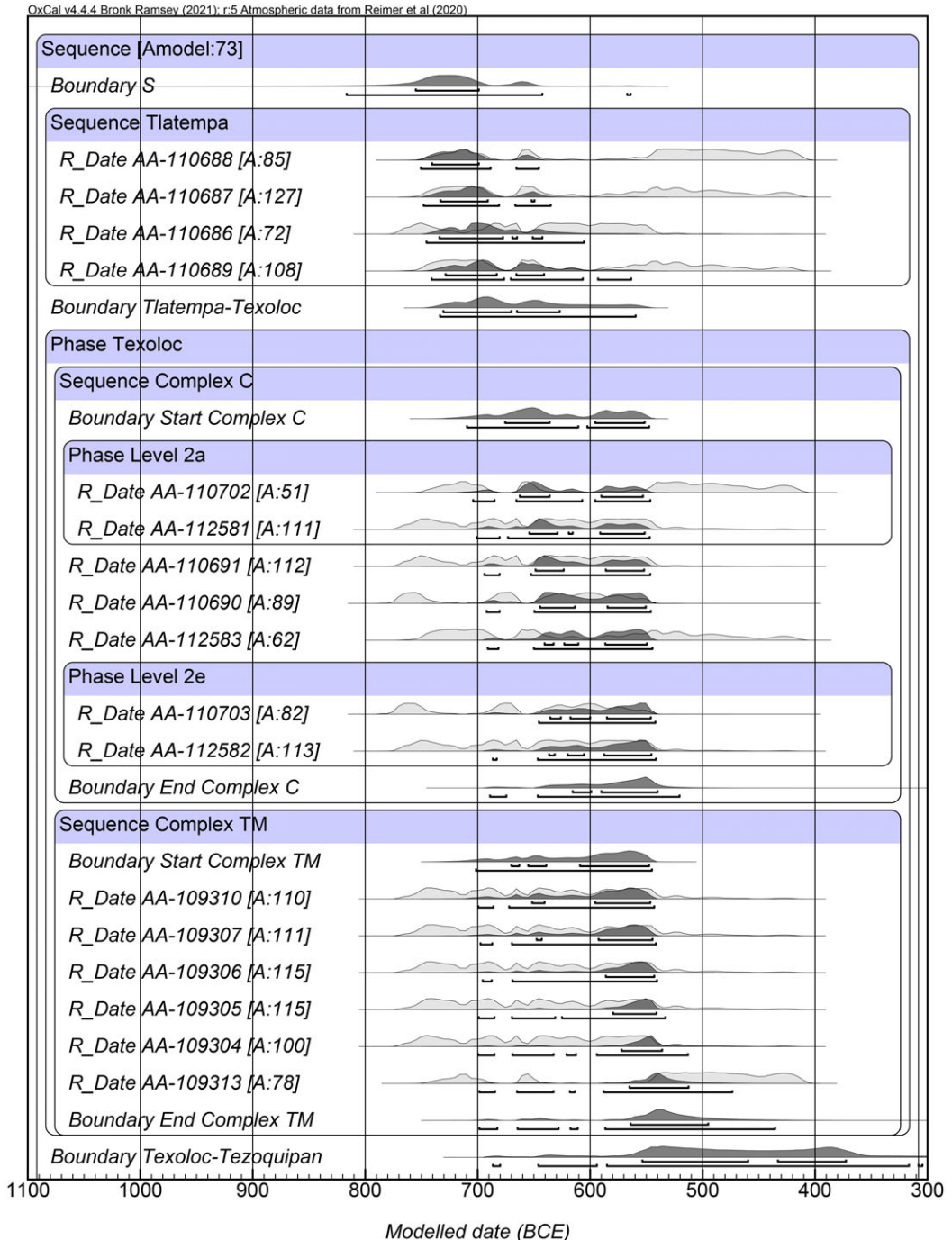
**Figure 7.** *Bayesian Model 8 (Overlapping Sequence method for both complexes) of the Middle Formative period at Tlalancaleca (Tezoquipan phase is not shown). Horizontal bars under the distributions are at 1σ and 2σ probability ranges.*

of the Hallstatt Plateau, thus serving to define the end of the Texoloc phase. While there were no substantial variations across modes with respect to the end date of the Texoloc phase, the mean values from models using samples from the Tres Marias Complex were consistently younger than the mean
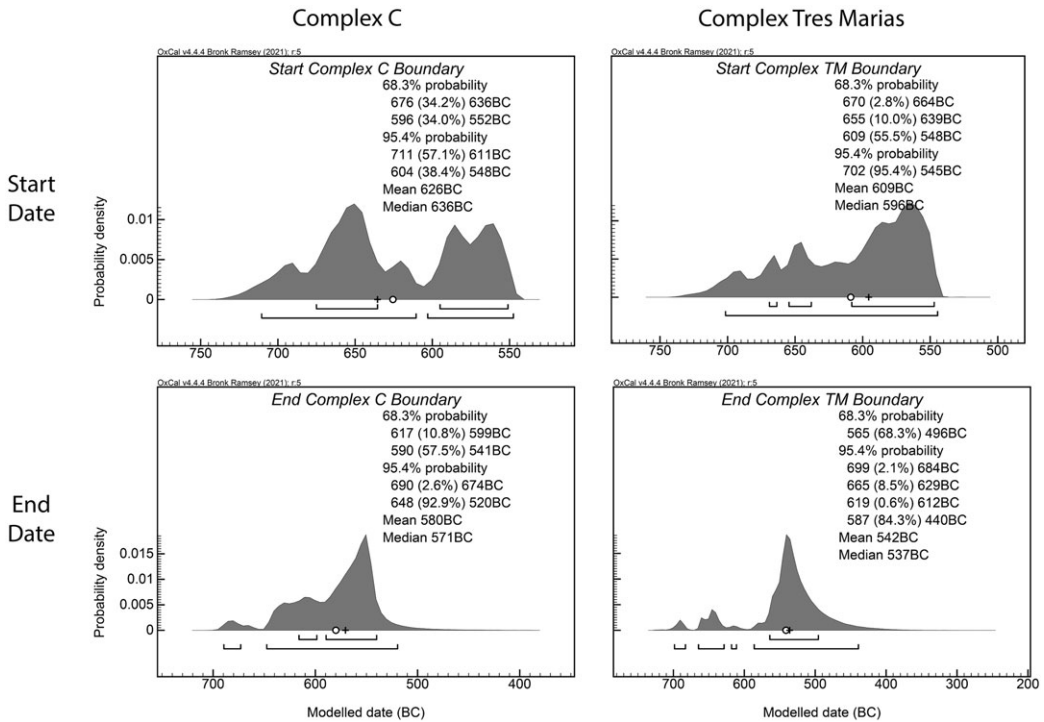
**Figure 8.** *Start and end dates of the Texoloc sequence for Complex C (left) and Complex Tres Marias (right) within Model 8 (Overlapping Sequence method for both complexes). Horizontal bars under the distributions are at 1σ and 2σ probability ranges.*

values of models based on samples from Complex C (Table 5). We also see this in the overlapping sequences between the two complexes in Model 8 (Figures 7 and 8). So, while there was certainly substantial overlap between the two complexes, it appears that data from Complex C served best to define the start of the Texoloc phase while data from the Tres Marias Complex served to estimate its end date. The most likely start date of Complex C's sequence of Texoloc samples (not the Texoloc phase) in Model 8 is around 650 cal BC (Figure 7) and we think our current data support this interpretation, though we cannot fully discard the possibility that the Texoloc phase started as early as 700 cal BC.

Given that the start and end dates of the Texoloc phase represent our estimates based on currently available evidence, it is crucial to analyze their uncertainties. Each model shows the 1σ and 2σ ranges for phase transitions (Tlatempa-Texoloc in Table 4; Texoloc-Tezoquipan in Table 5) and this allows us to compare the most probable ranges across models. The most probable 1σ ranges for the Tlatempa-Texoloc transition (where the central mode is located) vary from 35 years (661–626 cal BC) in Model 5 to as high as 105 years (731–626 cal BC) in Model 8; the mean of these ranges across models is 59.78 years and the median range is 47 years. We can consider the Tlatempa-Texoloc transition date using the mean value, assuming all models carry some validity. The average of means across the contiguous models is 661 cal BC with a standard deviation of ±17 years (means are more or less normally distributed). The standard error of the mean is 5.6 and the 95% confidence interval is 674-648 cal BC or ±13 years from the mean (numbers are rounded). We also calculated 95% credible intervals using Bayesian statistics with IBM® SPSS® Statistics 27. The result was 677–645 cal BC or ±16 years from the mean (numbers are rounded). Considering all of these probable ranges, we conclude that our uncertainties for the Tlatempa-Texoloc transition date are on a scale of 30 years (or ±15 years) or so.

For the Texoloc-Tezoquipan boundary, the 1σ range varies from 67 years (575–508 cal BC) in Model 1 to 144 years (592–448 cal BC) in Model 2. The mean of these ranges across the models is 102 years and the median is 94 years (i.e. around ±50 years). The mean average is 516 cal BC with a

standard deviation of ±38 years. The standard error is 12.7 and the 95% confidence interval is 545–487 cal BC or ±29 years from the mean. The Bayesian 95% credible interval is 552-480 cal BC or ±36 years from the mean. Our estimate of the Texoloc-Tezoquipan transition date, therefore, is less certain with uncertainties on a scale of 60–80 years (or ±30 to ±40 years). This is due to the small size of Early Tezoquipan samples and so future research will need to obtain more Early Tezoquipan samples to remedy this limitation.

## Summary

In summary, our analyses suggest the Texoloc phase began around 650 cal BC and lasted approximately 150 years, ending around 500 cal BC. Our work corroborates the latest revision of the Formative period chronology in central Tlaxcala by Lesure and colleagues (2006, 2014). They proposed that the Texoloc phase spanned 650 to 500 cal BC based on radiocarbon dates and ceramic cross-dating with the Basin of Mexico. Such work (including that of Tolstoy 1978) marked an important advance in refining the Middle Formative chronology and point of departure for future study. Murakami (2022) recently corroborated their proposed date of 650 cal BC for the Zacatenco-Ticoman transition by recalibrating published dates from the Basin of Mexico and Bayesian modeling. The current study builds on this collection of work, analyzing for the first time the Tlatempa-Texoloc transition based on data with direct stratigraphic superposition. Concordant results between these independent projects provides a strong basis for chronology building in Central Mexico.

The point-estimate for phase transition dates in chronology building is commonplace but we need to be cautious about its use (e.g., Telford et al. 2004). Its ubiquity reflects archaeologists' conception of archaeological phases as discrete spatio-temporal entities (Cowgill 1996), which is fitting for transitions that were presumably abrupt. However, phase transitions could also occur gradually, in which case they are better regarded as a range without clear boundaries. If this was the case, transitions should be examined through independent lines of evidence, such as careful observations of stratigraphy and ceramic seriation. Our impression is that the Tlatempa-Texoloc transition corresponds well to construction activities at Compound C7 and the Tres Marias Complex, but we will continue to verify this further during future research.

## Conclusion

Bayesian modeling of radiocarbon dates from well-documented Tlatempa, Texoloc, and Tezoquipan levels supports the placement of the Texoloc phase at 650–500 cal BC. This phase marks the onset of population nucleation at Tlalancaleca and probably other sites in Central Mexico as well. The ceramics characteristic of the Tlatempa, Texoloc, and Tezoquipan phases have been documented at Xochitécatl (Serra Puche et al. 2004), Totimehuacán (Spranz 1970), Amalucan (Fowler 1987), Cuauhtinchan Viejo (Seiferle-Valencia 2007), and La Laguna (Carballo 2016) among other centers (see Plunket and Uruñuela 2005; 2012 for an overview of the Puebla-Tlaxcala Valley). Ceramics of the contemporaneous phases (Zacatenco and Ticoman) in the Basin of Mexico have been reported at Cuicuilco (Heizer and Bennyhoff 1972; Muller 1990) and Tlapacoya (Barba de Piña Chán 1980; Niederberger 1976) among others (see Sanders et al. 1979 for general overview). Scholars agree that these sites were mid- to large-scale urban centers during the Late Formative period and whose origins likely lay in the Middle Formative. That "great towns" or "cities" (García Cook 1981, 257) were established concurrently, and ceramics changed concordantly in the Basin of Mexico and Puebla-Tlaxcala Valley during the Texoloc phase implies processes of social transformation that were macroregional in scale, although there might have been temporal variations in the timing of initial population nucleation and subsequent urban transformations. To date, the internal chronologies at many of these sites are not well established or complicated by a fragmentary archaeological record. That early work focused on monumental structures only narrowed further the window from which to understand trajectories of urban development. Tlalancaleca represents perhaps the only case where the internal chronology is relatively well-

established and diachronic settlement changes are mapped. This study has corroborated and highlighted the short duration of the Texoloc phase (150 years instead of 450 years as initially proposed by García Cook). By implication, the process of population nucleation at Tlalancaleca was a much more rapid process than previously thought. Future research will need to confirm whether processes of population nucleation were equally rapid at other sites.

# References

Barba de Piña Chán B (1980) *Tlapacoya: Los principios de la teocracia en la Cuenca de México*. Mexico City: Biblioteca Enciclopedica del Estado de México.

Bayliss A (2007) Bayesian buildings: An introduction for the numerically challenged. *Vernacular Architecture* **38**, 76–87.

Bayliss A, Bronk Ramsey C, van der Plicht J and Whittle A (2007) Bradshaw and Bayes: Towards a timetable for the Neolithic. *Cambridge Archaeological Journal* **17**(1), 1–28.

Beramendi-Orosco LE, Gonzalez-Hernandez G, Urrutia-Fucugauchi J, Manzanilla LR, Soler-Arechalde AM, Goguitchaishvili A and Jarboe N (2009) High-resolution chronology for the Mesoamerican urban center of Teotihuacan derived from Bayesian statistics of radiocarbon and archaeological data. *Quaternary Research* **71**, 99–107.

Bronk Ramsey C (1995) Radiocarbon calibration and analysis of stratigraphy: The OxCal program. *Radiocarbon* **37**(2), 425–430.

Bronk Ramsey C (2009a) Dealing with outliers and offsets in radiocarbon dating. *Radiocarbon* **51**, 1023–1045.

Bronk Ramsey C (2009b) Bayesian analysis of radiocarbon dates. *Radiocarbon* **51**, 337–360.

Bronk Ramsey C (2017) Methods for summarizing radiocarbon datasets. *Radiocarbon* **59**(2), 1809–1833.

Buck CE (2001) Application of the bayesian statistical paradigm. In Brothwell DR and Pollard AM (eds), *Handbook of Archaeological Sciences*. Chichester, UK: John Wiley & Sons, Ltd., 695–702.

Buck CE, Litton CD and Smith AFM (1992) Calibration of radiocarbon results pertaining to related archaeological events. *Journal of Archaeological Science* **19**(5), 497–512.

Burr GS, Donahue DJ, Tang Y, Beck JW, McHargue L, Biddulph D, Cruz R and Jull AJT (2007) Error analysis at the NSF-Arizona AMS facility. *Nuclear Instruments and Methods in Physics Research B* **259**, 149–153.

Carballo DM (2016) *Urbanization and Religion in Ancient Central Mexico*. Oxford: Oxford University Press.

Christen JA (1994) Summarizing a set of radiocarbon determinations: A robust approach. *Journal of the Royal Statistical Society. Series C (Applied Statistics)* **43**(3), 489–503.

Cowgill GL (1996) Discussion. *Ancient Mesoamerica* **7**, 325–331.

Donahue DJ, Jull AJT and Toolin LJ (1990) Radiocarbon measurements at the University of Arizona AMS facility. *Nuclear Instruments and Methods in Physics Research Section B* **52**(3–4), 224–228.

Fowler ML (1987) Early water management at Amalucan, state of Puebla, Mexico. *National Geographic Research* **3**(1), 52–68.

García Cook A (1972) Investigaciones arqueológicas en el estado de Tlaxcala. *Comunicaciones* **6**, 21–26.

García Cook A (1974) Una secuencia cultural para Tlaxcala. *Comunicaciones* **10**, 5–22.

García Cook A (1976) El Proyecto Puebla-Tlaxcala: Orígen, finalidad y logros. *Comunicaciones* Suplento III, 5–12.

García Cook A (1981) The historical importance of Tlaxcala. In Bricker V and Sabloff JA (eds), *Supplement to the Handbook of Middle American Indians, Vol 1: Archaeology*. Austin: University of Texas Press, 244–276.

García Cook A and Merino Carrión BL (1997) Notas sobre la cerámica prehispánica en Tlaxcala. In García Cook A and Merino Carrión BL, editors. *Antología de Tlaxcala, Vol 4*. Mexico City: Instituto Nacional de Antropología e Historia, 161–230.

García Cook A and Merino Carrión BL (2005) La cerámica del Formativo en Puebla-Tlaxcala. In Merino Carrión BL and García Cook Á (eds), *La Producción Alfarera en el México Antiguo I*. Mexico City: Instituto Nacional de Antropología e Historia, 575–685.

Grove DC (2000) The Preclassic societies of the central highlands of Mesoamerica. In Adams REW and Macleod MJ (eds). *The Cambridge History of the Native Peoples of the Americas Volume II: Mesoamerica, Part 1*. Cambridge: Cambridge University Press, 122–155.

Hamilton D and Krus A (2018) The myths and realities of Bayesian Chronological Modeling revealed. *American Antiquity* **83**(2), 187–203.

Heizer RF and Bennyhoff J (1972) Cuicuilco México, 1957. *National Geographic Society Research Report* **1955–1960**, 93–104.

Jacobsson P, Hamilton WD, Cook G, Crone A, Dunbar E, Kinch H, Naysmith P, Tripney B and Xu S (2018) Refining the Hallstatt plateau: Short-term ^{14}C variability and small scale offsets in 50 consecutive single tree-rings from southwest Scotland dendro-dated to 510–460 BC. *Radiocarbon* **60**(1), 219–237.

Kus AM and Cobb CR (2018) The Mississippian fin de siècle in the Middle Cumberland region of Tennessee. *American Antiquity* **83**(2), 302–319.

Lesure RG, Borejsza A, Carballo J, Frederick C, Popper V and Wake TA (2006) Chronology, subsistence, and the earliest Formative of central Tlaxcala, Mexico. *Latin American Antiquity* **17**(4), 474–492.

Lesure RG, Carballo J, Carballo DM, Borejsza A and Rodríguez López I (2014) A Formative chronology for central Tlaxcala. In Lesure RG (ed), *Formative Lifeways in Central Tlaxcala: Volume 1: Excavations, Ceramics, and Chronology*. University of California, Los Angeles: Cotsen Institute of Archaeology Press, 315–362.

Manning SW, Bronk Ramsey C, Kutschera W, Higham T, Kromer B, Steier P and Wild EM (2006) Chronology for the late Bronze age 1700–1400 B.C. *Science* **312**, 565–569.

McDonald L and Manning SW (2023) A simulation approach to quantify the parameters and limitations of the radiocarbon wiggle-match dating technique. *Quaternary Geochronology* **75**, 101423.

Michczyńska A and Michczyńska DJ (2006) The effect of PDF peaks' height increase during calibration of radiocarbon date sets. *Geochronometria* **25**, 1–4.

Muller F (1990) *La Cerámica de Cuicuilco B: Un Rescate Arqueológico*. Mexico City: Instituto Nacional de Antropología e Historia.

Murakami T (2022) Refining the Middle Formative chronology in Central Mexico: Implications for the origins of the Central Mexican urban tradition. In Santasilia CE, Hepp GD and Diehl RA (eds), *Identities, Experience, and Change in Early Mexican Villages*. Gainesville: University Press of Florida, 224–257.

Murakami T and Kabata S (eds) (2019) *Informe técnico de la séptima temporada del Proyecto Arqueológico Tlalancaleca, Puebla*. Mexico City: Archive of Instituto Nacional de Antropología e Historia.

Murakami T, Kabata S and López JM (eds) (2017b) *Informe técnico de la quinta temporada del Proyecto Arqueológico Tlalancaleca, Puebla*. Mexico City: Archive of Instituto Nacional de Antropología e Historia.

Murakami T, Kabata S and López JM (eds) (2018) *Informe técnico de la sexta temporada del Proyecto Arqueológico Tlalancaleca, Puebla*. Mexico City: Archive of Instituto Nacional de Antropología e Historia.

Murakami T, Kabata S, López J JM and Chávez V JJ (2017a) Development of an early city in Central Mexico: The Tlalancaleca archaeological project. *Antiquity* **91**, 455–473.

Niederberger C (1976) *Zohapilco: Cinco milenios de ocupacion humana en un sitio lacustre de la cuenca de Mexico*. Mexico City: Instituto Nacional de Antropología e Historia.

Plunket P and Uruñuela G (2005) Recent research in Puebla prehistory. *Journal of Archaeological Research* **13**(2), 89–127.

Plunket P and Uruñuela G (2012) Where east meets west: The Formative in Mexico's central highlands. *Journal of Archaeological Research* **20**, 1–51.

Reimer P, Bard E, Bayliss A, Beck JW, Blackwell PG, Bronk Ramsey C, Buck CE, Cheng H, Edwards RL, Friedrich M et al. (2013) IntCal13 and Marine 13 radiocarbon age calibration curves 0–50,000 years cal BP. *Radiocarbon* **55**(4), 1869–1887.

Reimer PJ, Austin WEN, Bard E, Bayliss A, Blackwell PG, Ramsey CB, Butzin M, Cheng H, Edwards RL, Friedrich M et al. (2020) The IntCal 20 Northern Hemisphere radiocarbon age calibration curve (0–55 cal kbp). *Radiocarbon* **62**(4), 725–757.

Sanders WT, Parsons JR and Santley RS (1979) *The Basin of Mexico: Ecological processes in the evolution of a civilization*. New York: Academic Press.

Seiferle-Valencia AC (2007) Before the eagle's nest: The Formative period archaeology of Cuauhtinchan Viejo, Puebla, Mexico. PhD dissertation, Cambridge: Harvard University.

Serra Puche MC, Arce JCL and De La Torre Mendoza M (2004) *Cerámica de Xochitécatl*. Mexico City: Instituto de Investigaciones Antropológicas, Universidad Nacional Autónoma de México.

Snow DR (1969) Ceramic sequence and settlement location in prehispanic Tlaxcala. *American Antiquity* **34**(2), 131–145.

Spranz B (1970) *Die pyramiden von Totimehuacan, Puebla (Mexico)*. Wiesbanden, Germany: Franz Steiner Verlag.

Steier P and Rom W (2000) The use of bayesian statistics for ^{14}C dates of chronologically ordered samples: A critical analysis. *Radiocarbon* **42**(2), 183–198.

Telford RJ, Heegaard E and Birks HJB (2004) The intercept is a poor estimate of a calibrated radiocarbon age. *Holocene* **14**(2), 296–298.

Tolstoy P (1978) Western Mesoamerica before A.D. 900. In Taylor RE and Meighan CW (eds), *Chronology in New World Archaeology*. New York: Academic Press, 241–284.

Tsukamoto K, Tokanai F, Moriya T and Nasu H (2020) Building a high-resolution chronology at the Maya archaeological site of El Palmar, Mexico. *Archaeometry* **62**(6), 1235–1266.